Journal of Chromatography, 506 (1990) 185–200
Elsevier Science Publishers B.V., Amsterdam — Printed in The Netherlands

CHROMSYMP. 1782

Theoretical optimization of open-tubular columns for liquid chromatography with respect to mass loadability

P. P. H. TOCK*, P. P. E. DUIJSTERS, J. C. KRAAK and H. POPPE
Laboratory of Analytical Chemistry, University of Amsterdam, Nieuwe Achtergracht 166, 1018 WV Amsterdam (The Netherlands)

SUMMARY

A procedure is described for designing open-tubular liquid chromatographic (LC) columns with high resolving power, optimized for mass loadability. Large film thicknesses improve the loadability, but decrease the efficiency owing to the increased mass-transfer term. Normally an arbitrary upper limit of the magnitude of the contribution of the stationary phase mass-transfer term to the overall plate-height equation of about 20% is accepted. The present approach allows the real optimum value of the contribution of the stationary phase mass-transfer term to be calculated. The optimum was found to occur at about 50% in most instance. This corresponds to a plate height equation $h = 2/v + 0.12v$ for $k' = 3$ instead of the expression for very thin films $h = 2/v + 0.08v$ as advocated by Knox and Gilbert (h = reduced plate height, v = reduced velocity; k' = capacity factor). The maximum column length is about 5 m for all phase systems with $3 \cdot 10^5$ theoretical plates, dead time of mobile phase 1000 s and 20 MPa pressure drop along the column. The mass loadability of an open-tubular LC column and a 21-μm micropacked capillary were compared and were found to be in the same range. The optimization procedure uses known and established relationships, describing speed, efficiency and mass loadability in chromatographic systems. The calculations were carried out with a spreadsheet computer program.

INTRODUCTION

Optimum resolving power and speed for open-tubular liquid chromatographic (LC) columns has been predicted for columns of I.D. 1–5 μm[1,2]. It has been shown that the theoretical predicted optimum resolving power can be realized in practice[3–14]. Various stationary layers or films can now be coated successfully in 5-μm (and larger) fused-silica capillaries with near to the theoretical performance[6–12]. The excellent performance can only be realized by keeping the external band broadening in these systems below 1 nl. The requirements on the external band broadening can be achieved by applying on-column detection[4,5] and split-injection techniques[3,11]. However, these required extremely small volumes, implying a dramatic decrease in concentration detectability of the solutes, which limits the dynamic range of the system. Improve-

0021-9673/90/$03.50 © 1990 Elsevier Science Publishers B.V.

ments in this respect can be achieved by increasing the mass loadability of open-tubular LC columns. This can be achieved by using larger inner diameters, which would be putting the cart before the horse in view of the increase in the transverse molecular diffusion term in the Golay equation[15], and by using thicker stationary phases. The latter also can only be increased to a certain limit, because of the accompanying increase in the stationary mass-transfer term in the Golay equation. Normally an arbitrary upper limit (*e.g.*, 20%) to the magnitude of the contribution of the stationary phase mass-transfer term relative to the overall plate height equation is accepted. However, whether this percentage represents the correct, *i.e.*, optimum, value is unkown. Therefore, it is of importance to develop an optimization strategy procedure in order to design columns with a high resolving power in a reasonable analysis time with high sample capacity.

We believe that columns optimized from this point of view offers more prospects in the near future. The better efficiency of open-tubular LC columns compared with packed columns has been proved, but for more practical use of open-tubular LC in the future, *e.g.*, outside research and university laboratories, it is necessary to demonstrate its real power with practical applications. In view of the large differences in concentrations that occur in such applications, a high dynamic range, and therefore a high column loadability, are essential. The present procedure gives the chromatographer an easy guideline to design such columns.

Many papers[16,17] have discussed the influence of various column parameters on loadability, efficiency and speed. Noy *et al.*[18] derived some equations which show the effect of column dimensions on the minimum detectable amount (for a mass flow-sensitive detector) and the minimum analyte concentration (for a concentration-sensitive detector).

Recently, Ghijsen and Poppe[19] reported an optimization procedure for designing capillary gas chromatographic (GC) columns with maximum loadability at a given performance in terms of efficiency and speed of separation and compared these columns with packed GC columns. They used a procedure based on known and established relationships describing plate height (Golay–Giddings)[20], speed (t_m according to Knox and Saleem)[2] and an estimate of mass loadability, M_{pl}, which is equal to the amount of stationary phase in one plate[21]. The calculations were carried out with a spreadsheet computer program, which ensured the user a large flexibility for selecting different specifications. Especially the flexibility attracted us to use this procedure to propose a new design of open-tubular LC columns.

The optimization procedure was carried out for three phase systems, the usefulness of which has been demonstrated in open-tubular LC: a porous silica layer with a liquid–liquid phase system[10–12], a cross-linked silicone phase system[6–10] and an adsorption system on a flat wall, which will henceforth be termed as liquid–liquid system, silicone system and monolayer system, respectively.

PROCEDURE

The optimization procedure was carried out following the flow chart in Fig. 1 (symbols are defined at the end of the paper). It starts with the input of the specifications (t_m, ΔP, N) and the exprimental constant (φ, η) to calculate h, using eqn. 1, which is a rearranged form of the well known equation of Knox and Saleem[2]. Once

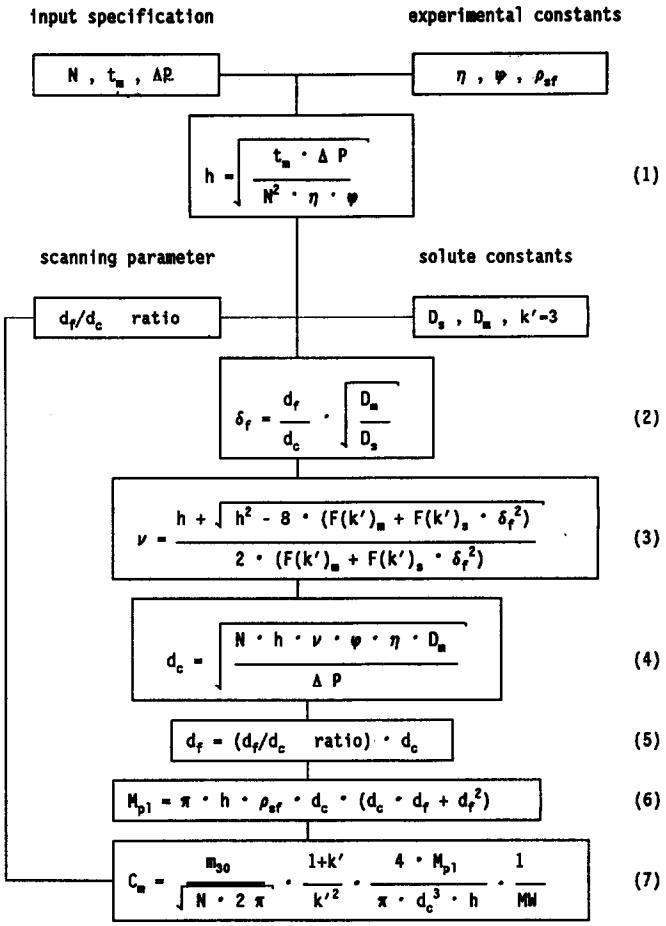

Fig. 1. Flow chart for the optimization procedure.

h is known, the value of ν, and with that the whole set of conditions, would be accessible, provided that the h–ν curve is available. Each value of the d_f/d_c ratio (the scanning parameter) corresponds to one particular h–ν plot, $h = 2/\nu + C\nu$, where $C = F(k')_m + F(k')_s\delta_f^2$ and δ_f is the reduced film thickness[22]:

$$F(k')_m = \frac{(1 + 6k' + 11k'^2)}{96(1 + k')^2}$$

$$F(k')_s = \frac{2k'}{3(1 + k')^2}$$

Scanning the value of d_f/d_c yields a set of solutions to the problem. The derivation of the h–ν curve in each instance proceeds via δ_f, calculated with eqn. 2 substituting D_s, D_m, $k' = 3$ and the ratio d_f/d_c. The definition of d_f and d_c can be seen in Fig. 2. The

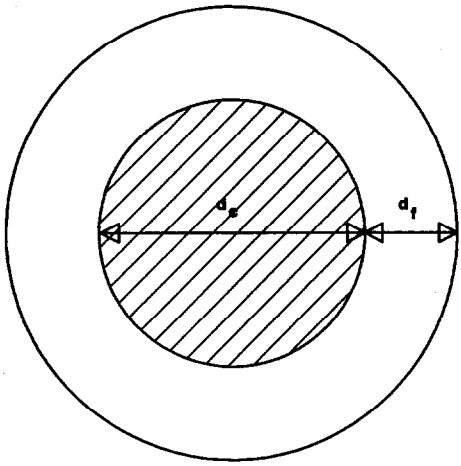

Fig. 2. Definition of the inner diameter and film thickness as used in the optimization procedure.

value of δ_f was then substituted in the rearranged dimensionless Golay–Giddings equation[20] (eqn. 3), to obtain the h–v function and v (taking the larger root). Next d_c was calculated with eqn. 4, the Poiseuille equation.

Once a whole set of columns, each with a δ_f value, but all of them satisfying the speed and efficiency requirements, have been found, the one with the highest mass loadability, M_{pl}, can be selected. As a criterion to do that, the amount of stationary phase (either surface area or volume/mass) was used, in accordance with the theoretical[21] and the exprimental evidence[23,24], showing that this is a good measure of loadability. Finally, d_f, M_{pl} and C_m, the eluting concentration which is the outlet concentration of the solute in the mobile phase, were calculated using eqns. 5, 6 and 7, respectively.

The d_f/d_c ratio was varied from 0 to 3 in steps of 0.05 for the liquid–liquid system and from 0 to 0.3 in steps of 0.005 for the silicone system. The obtained values of M_{pl}, d_c, d_f, $d_c + 2d_f$, L and C_m were plotted against the d_f/d_c ratio for different specifications, *e.g.*, varying one specification while the others remained fixed.

RESULTS AND DISCUSSION

The optimization procedure in Fig. 1 was applied to the liquid–liquid system and the silicone system. The d_f/d_c ratio was used as the scanning parameter and the fixed input specifications were $N = 3 \cdot 10^5$, $t_m = 1000$ s and $\Delta P = 20$ MPa. For the monolayer system, where the d_f/d_c ratio cannot be used, ΔP was used as the scanning parameter. The optimization procedure for the different specifications, different phase systems and the corresponding figures are summarized in Table I.

In the figures some d_f/d_c ratios have been marked with an asterisk; for these points the specifications can only be realized in the minimum of the h–v curve. Larger d_f/d_c ratios are inaccessible, because v cannot be calculated in eqn. 3 (Fig. 1) with the input specifications; the determinant of this equation is negative. The explanation of this fact is that for the d_f/d_c ratios marked with an asterisk h_{min} of the corresponding

TABLE I

CHARACTERISTICS OF THE OPTIMIZATION

Phase system[a]	$N \cdot 10^5$	t_m *(s)*	ΔP *(MPa)*	*Fig.*	*Remarks*
LL	3	1000	Variable	3a	M_{pl}–d_f/d_c ratio
LL	3	Variable	20	3b	M_{pl}–d_f/d_c ratio
LL	Variable	1000	20	3c	M_{pl}–d_f/d_c ratio
S	3	1000	Variable	4	M_{pl}–d_f/d_c ratio
M	3	Variable	*x*-axis	5	M_{pl}–ΔP
LL	3	1000	20	6a	Column dimensions
S	3	1000	20	6b	Column dimensions
LL	Variable	1000	20	7a	C_m–d_f/d_c ratio
S	Variable	1000	20	7b	C_m–d_f/d_c ratio
LL/S	*x*-axis	1000	20	8	Maximum M_{pl}–N
LL/S	*x*-axis	1000	20	9	C_m^{opt}–N

[a] LL = Liquid–liquid system, $D_s = 5 \cdot 10^{-10}$ m²/s; S = silicone system, $D_s = 7 \cdot 10^{-12}$ m²/s; M = monolayer system.

h–v curve is equal to the defined h, calculated with eqn. 1 (Fig. 1). For a larger d_f/d_c ratio, h_{min} of the corresponding h–v curve increases, *e.g.*, h_{min} is larger than the specified h, and therefore no v can be found on the h–v curve for the specified h. Inaccessible points are indicated with an asterisk in all figures.

Liquid–liquid system

In Fig. 3a, the calculations were made for various pressure drops in the range 2–100 MPa. It can be seen that the d_f/d_c ratio for the maximum M_{pl} decreases with increasing ΔP, but for $\Delta P = 40$ MPa or higher the optimum d_f/d_c ratio approaches a value $d_f/d_c = 0.485$. For the fixed input specifications the plate-height equation is $h = 2/v + 0.133v$; there is an increase in C of *ca.* 60% compared with columns with a very thin film. The column dimensions for the maximum M_{pl} at 20 and 40 MPa are listed in Table II. From these data it can be seen that doubling ΔP from 20 to 40 MPa hardly changes the column dimensions, but M_{pl} increase 1.4-fold. At high allowed pressure drops, *i.e.*, when a sizeable film thickness is possible, the loadability is indeed in general proportional to the square root of the inlet pressure.

In Fig. 3b, the calculations were made for various t_m values and it can be seen that the d_f/d_c ratio for maximum M_{pl} again increases to 0.485 with increasing t_m. The value of M_{pl} increases by a factor of 4 on doubling t_m, whereas the column dimensions show an increase of d_c, d_f, $d_c + 2d_f$ and L (Table II).

In Fig. 3c, the calculations were made for various N values and it can be seen that the d_f/d_c ratio for maximum M_{pl} increases only from 0.475 for $N = 3 \cdot 10^5$ to 0.495 for $N = 1 \cdot 10^5$. In this instance M_{pl} increases 16.5-fold, whereas d_c and L increase by the square root of 3 and d_f increases 1.8-fold (Table II).

As an example, these calculations show that when a plate number of $3 \cdot 10^5$ is needed, a pressure drop of 20 MPa can be allowed in combination with a dead time of 1000 s (an analysis time of 4000 s), and with maximum loadability this will result in the following column system: coat a 3.9 m × 9.6 μm I.D. capillary with a porous support

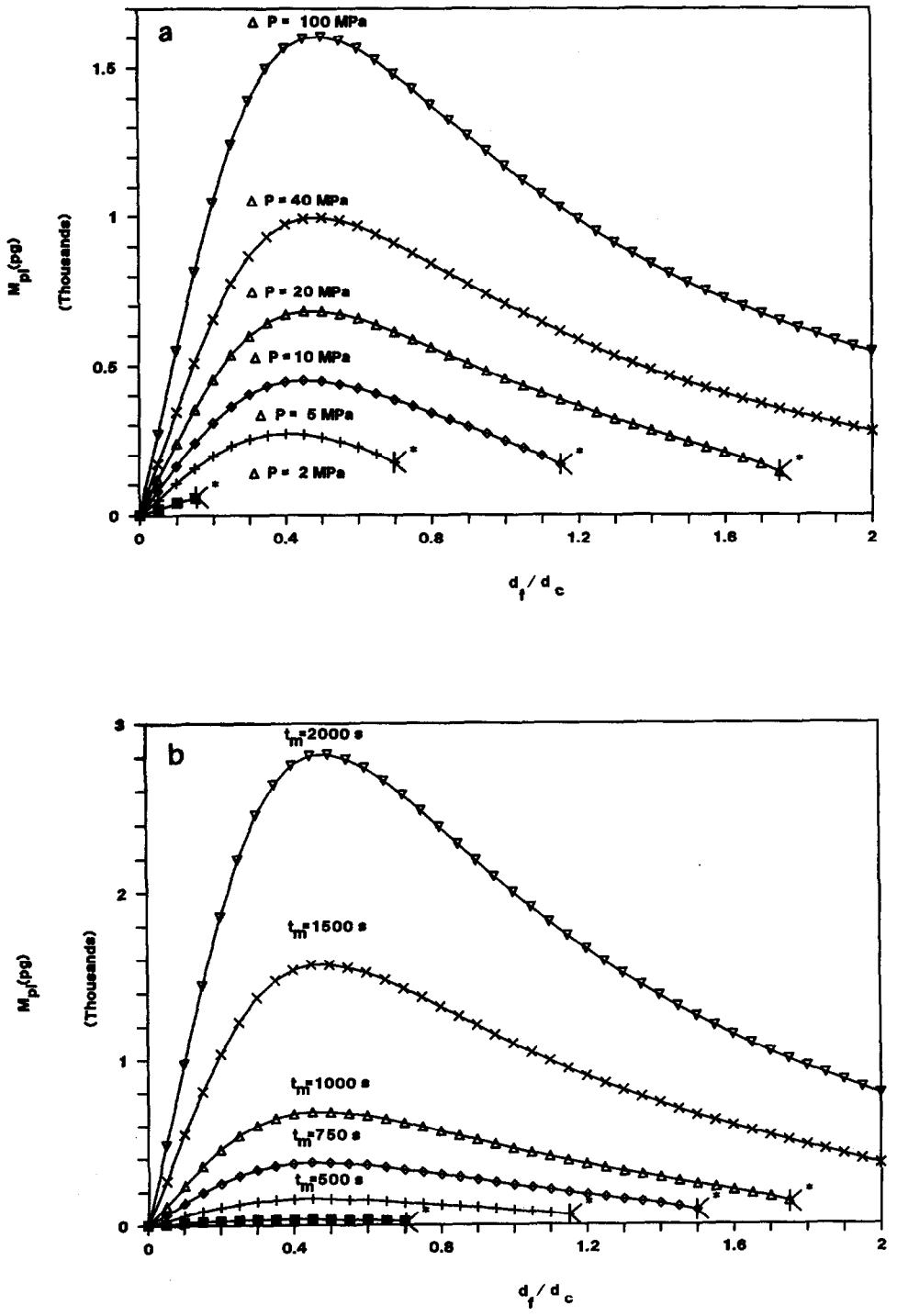
a
Δ P = 100 MPa
Δ P = 40 MPa
Δ P = 20 MPa
Δ P = 10 MPa
Δ P = 5 MPa
Δ P = 2 MPa
M_{pl} (pg)
(Thousands)
d_f / d_c
b
t_m=2000 s
t_m=1500 s
t_m=1000 s
t_m=750 s
t_m=500 s
M_{pl} (pg)
(Thousands)
d_f / d_c

Fig. 3.

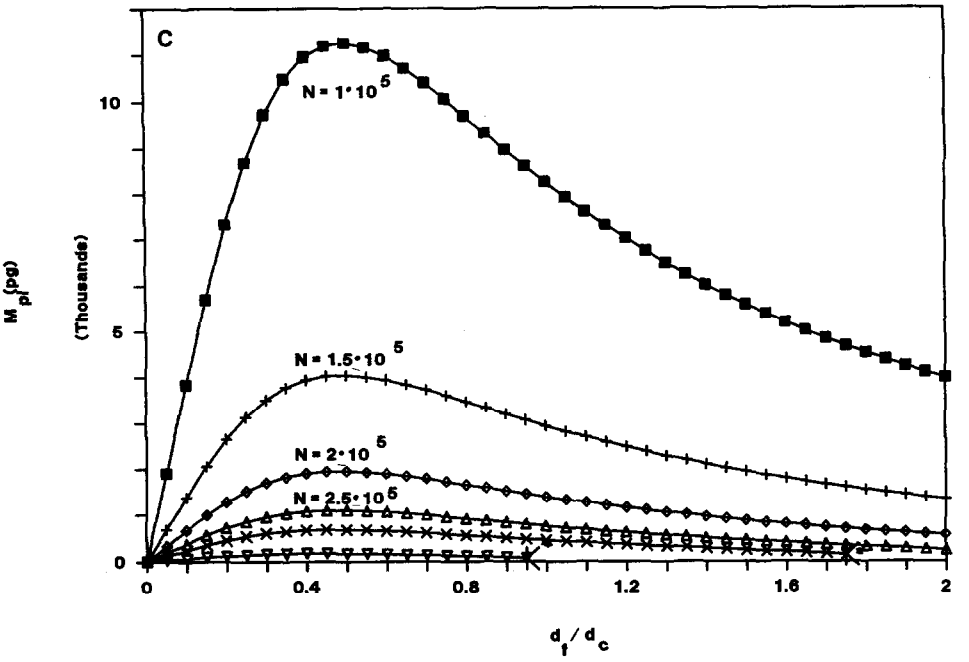

Fig. 3. Mass loadability M_{pl} (pg) *versus* d_f/d_c ratio for the liquid–liquid system. (a) $N = 3 \cdot 10^5$, $t_m = 1000$ s and various ΔP values: ■ = 2; + = 5; ◇ = 10; △ = 20; × = 40; ▽ = 100 MPa. (b) $N = 3 \cdot 10^5$, $\Delta P = 20$ MPa and various t_m values: ■ = 250; + = 500; ◇ = 750; △ = 1000; × = 1500; ▽ = 2000 s. (c) $t_m = 1000$ s, $\Delta P = 20$ MPa and various N values: ■ = $1 \cdot 10^5$; + = $1.5 \cdot 10^5$; ◇ = $2 \cdot 10^5$; △ = $2.5 \cdot 10^5$; × = $3 \cdot 10^5$; ▽ = $5 \cdot 10^5$.

layer and generate on this column a liquid–liquid system with a film thickness of 2.3 μm. The maximum loadability will be 680 pg of a solute with $k' = 3$. From Fig. 3a–c for the liquid–liquid system the following conclusions can be drawn: changes in N and t_m have a very strong and strong influence, respectively, on M_{pl}; changes in ΔP has a weak influence on M_{pl}, approximately by $\sqrt{\Delta P}$; the arbitrary upper limit of a 20% increase in C is an acceptable limit, but at maximum M_{pl} for the liquid–liquid system a 60% contribution of the mass-transfer term gives a better compromise; the plate height equation for the liquid–liquid system is $h = 2/v + 0.133v$; and M_{pl} increases, as expected, with a decrease in efficiency or with an increase in analysis time or pressure drop.

Silicone system

The optimization procedure was also carried out with the silicone system. The resulting plots were similar to those for the liquid–liquid system. The dependences of M_{pl} on N, t_m and ΔP are identical for both phase systems, only the d_f/d_c ratio and the obtained M_{pl} values being different. In Fig. 4, which can be compared with Fig. 3a, it can be seen that M_{pl} and the d_f/d_c ratios are about ten times smaller for the silicone system than for the liquid–liquid system. This can be explained by the difference in the diffusion coefficients in the stationary phase for the two phase systems; in eqn. 2 (Fig. 1), δ_f depends on the square root of the diffusion coefficients. In Table II the column

TABLE II

COLUMN DIMENSIONS AT MAXIMUM LOADABILITY

Phase system[a]	*Input specifications*					*Column dimensions*						*Fig.*
	$N \cdot 10^5$	t_m *(s)*	ΔP *(MPa)*	d_f/d_c	C	d_c *(μm)*	d_f *(μm)*	d_b[b] *(μm)*	L *(m)*	M_{pl} *(pg)*	C_m *(mmol/l)*	
LL	3	1000	40	0.485	0.136	4.91	2.38	9.67	5.49	1000	9.33	3a
LL	3	1000	20	0.475	0.133	4.90	2.33	9.56	3.87	680	9.07	3a
LL	3	2000	20	0.485	0.136	6.94	3.37	13.67	7.76	2820	9.33	3b
LL	1	1000	20	0.495	0.138	8.49	4.20	16.90	6.71	11 000	15.7	3c
S	3	1000	40	0.0475	0.117	5.29	0.25	5.79	5.91	86	0.64	4
S	3	1000	20	0.0465	0.115	5.28	0.25	5.77	4.17	59	0.63	4
S	3	2000	20	0.0475	0.117	7.48	0.36	8.19	8.36	244	0.64	–
S	1	1000	20	0.0480	0.118	9.19	0.44	10.07	7.27	970	1.13	–
M	3	1000	20	0	0.08	6.51	0	6.51	5.15	0.3 fg	–	5
M	3	2000	20	0	0.08	9.26	0	9.26	10.36	0.8 fg	–	5

[a] LL = Liquid–liquid system; S = silicone system; M = monolayer system.

[b] $d_b = d_c + 2d_f$.

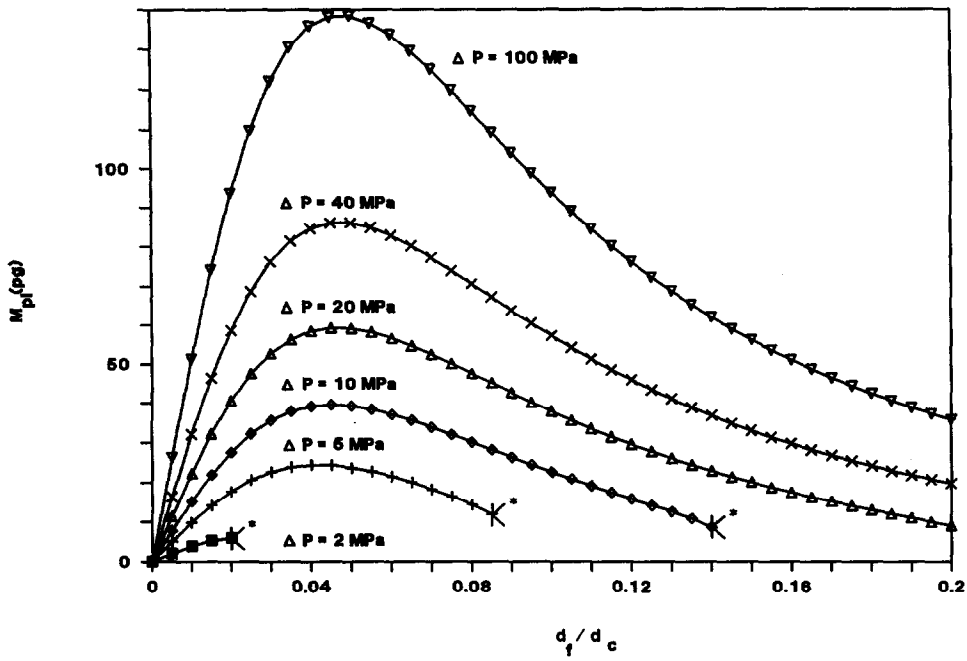

Fig. 4. Mass loadability M_{pl} (pg) *versus* d_f/d_c ratio for the silicone system with $N = 3 \cdot 10^5$, $t_m = 1000$ s and various ΔP values: ■ = 2; + = 5; ◇ = 10; △ = 20; × = 40; ▽ = 100 MPa.

dimensions for the maximum M_{pl} are listed and it can be seen that the main differences between the two phase systems are found in d_f and $d_c + 2d_f$, which amount to a factor of 10 and 1.7, respectively. The other column dimensions are almost the same. The plate-height equation for $\Delta P = 20$ MPa is $h = 2/v + 0.115v$, which is an increase in C of about 50%.

From Fig. 4, it can be concluded that: the use of a phase system with a very small diffusion coefficient in the stationary phase is, as expected, unfavourable with respect to mass loadability, roughly in proportion to the expression $\sqrt{(D_{s1}/D_{s2})}$, and the dependence of N, t_m and ΔP on M_{pl} is identical with that for the liquid–liquid system.

Monolayer system

The optimization procedure shown in Fig. 1 cannot be used for mass-loadability optimization for the monolayer system. The flow chart had to be changed, because the thickness of the monolayer cannot be varied and there is one degree of freedom less. The pressure drop ΔP was chosen as the scanning parameter with various t_m values and $N = 3 \cdot 10^5$. M_{pl} was calculated using the equation

$$M_{pl} = \pi h d_c^2 \mathrm{MW} \alpha_{OH(s)} \tag{8}$$

In Fig. 5 it can be seen that (i) M_{pl} is about $2 \cdot 10^6$ and $2 \cdot 10^5$ times smaller than in the liquid–liquid system and the silicone system, respectively, (ii) M_{pl} increases continuously with increasing ΔP and (iii) doubling t_m increases M_{pl} 2.7-fold (Table II). In Table II, the column dimensions for $\Delta P = 20$ MPa and $t_m = 1000$ and 2000 s are

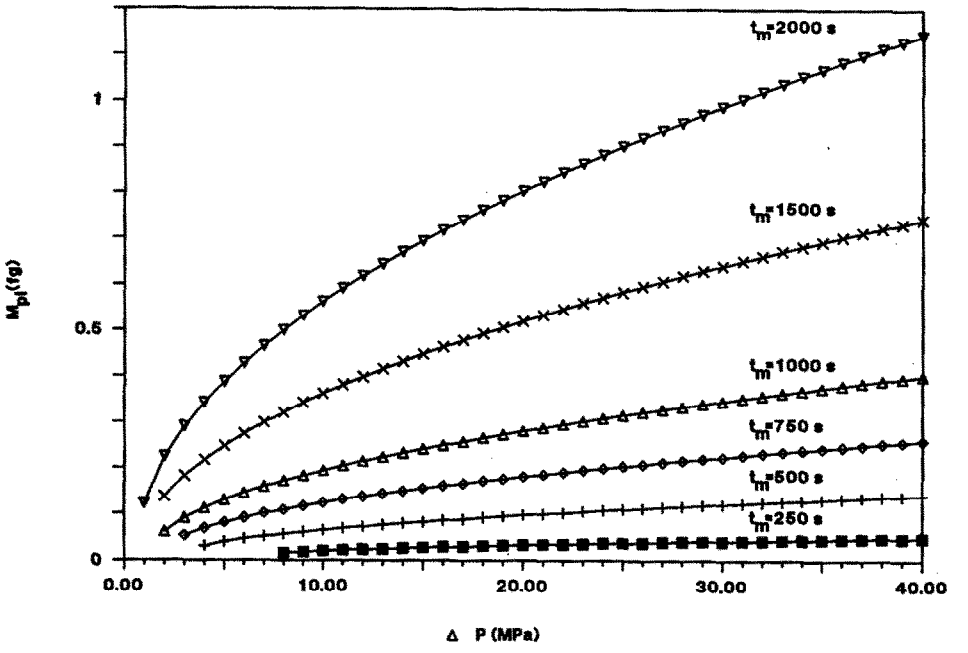

Fig. 5. Mass loadability M_{pl} (fg) *versus* ΔP for the monolayer systen with $N = 3 \cdot 10^5$ and for various t_m: ■ = 250; + = 500; ◇ = 750; △ = 1000; × = 1500; ▽ = 2000 s.

listed. L and d_c increase by the same factor on doubling t_m and are hardly different compared with the other phase systems. Finally, it can be noted that M_{pl} increases enormously if a stationary layer or film is applied in the capillary and therefore in our opinion columns should be prepared with stationary phases with suitable thickness.

Column dimensions

In Fig. 6a and b, the column dimensions for the liquid–liquid and silicone systems, respectively, are shown. It can be seen that the plots of L and d_c are almost identical for the two systems (except for the differing horizontal scales), whereas for d_f and $d_c + 2d_f$ a large difference is observed. The maximum length of the columns is about 5 m for the fixed input specifications. For the liquid–liquid system $d_c + 2d_f$ has a maximum at $d_f/d_c = 0.55$ and the maximum for d_f is at $d_f/d_c = 1.2$; for the silicone system these maxima are at $d_f/d_c = 0.01$ and 0.145, respectively.

Eluting concentration

In Fig. 1, C_m can be calculated with eqn. 7 and in Fig. 7a and b C_m is shown for the liquid–liquid and silicone system, respectively. The results of our calculations show that C_m can be influenced only by N and the d_f/d_c ratio, and not by ΔP and t_m. This can be explained by eqn. 7, in which C_m depends only on the reciprocal square root of N and the phase ratio, and the latter can be expressed as a function of d_f/d_c. The value of C_m varies in proportion to the reciprocal of the square root of N, and C_m increases continuously with increasing d_f/d_c. In Table II, C_m is listed at maximum M_{pl} and it can be seen that C_m is 14.4 times smaller for the silicone system than the liquid–liquid

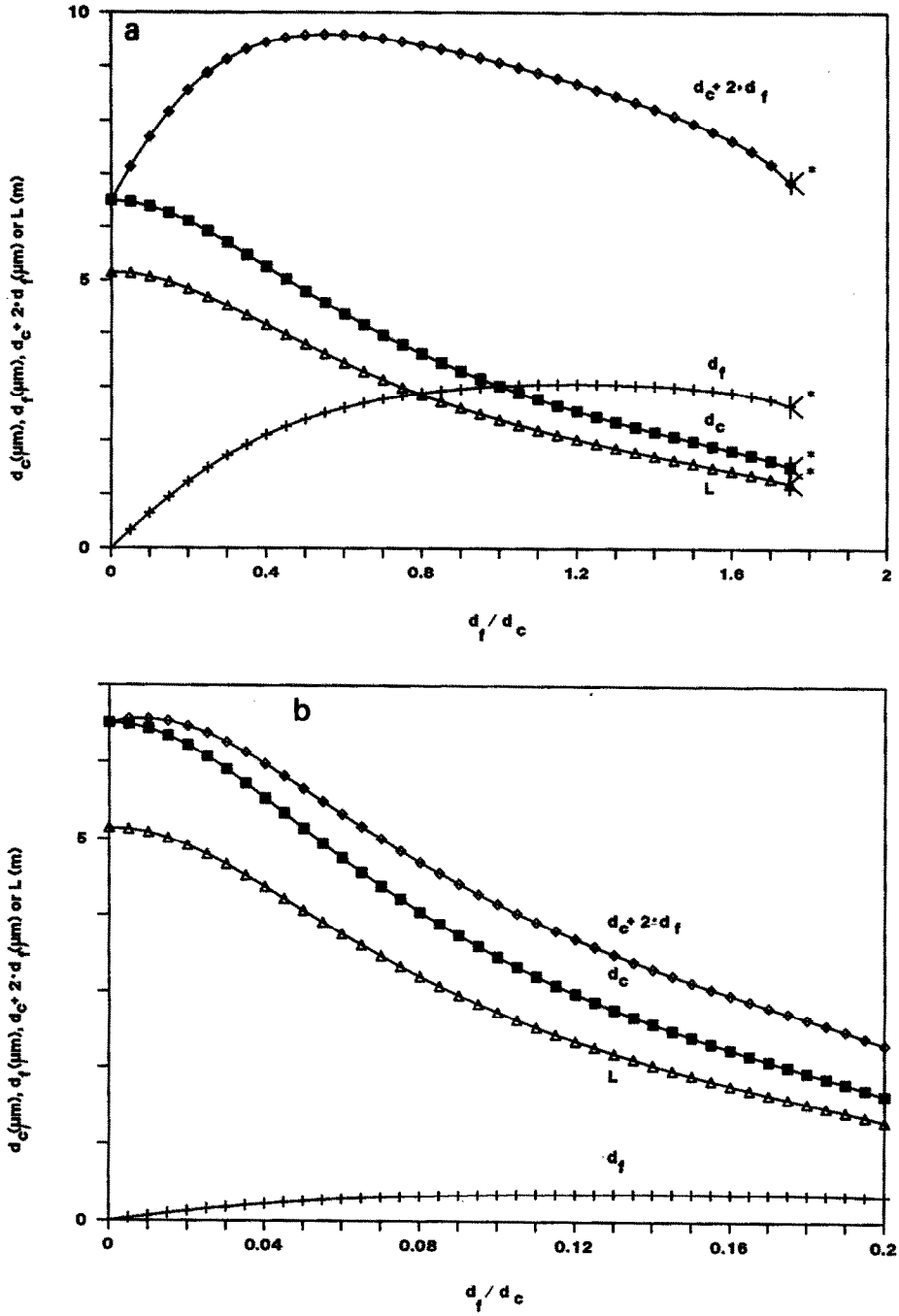

Fig. 6. Column dimensions *versus* d_f/d_c ratio. (a) For the liquid–liquid system with $N = 3 \cdot 10^5$, $t_m = 1000$ s and $\Delta P = 20$ MPa. ■ = d_c (μm); + = d_f (μm); ◇ = $d_c + 2d_f$ (μm); △ = L (m). (b) For the silicone system with $N = 3 \cdot 10^5$, $t_m = 1000$ s and $\Delta P = 20$ MPa. ■ = d_c (μm); + = d_f (μm); ◇ = $d_c + 2d_f$ (μm); △ = L (m).

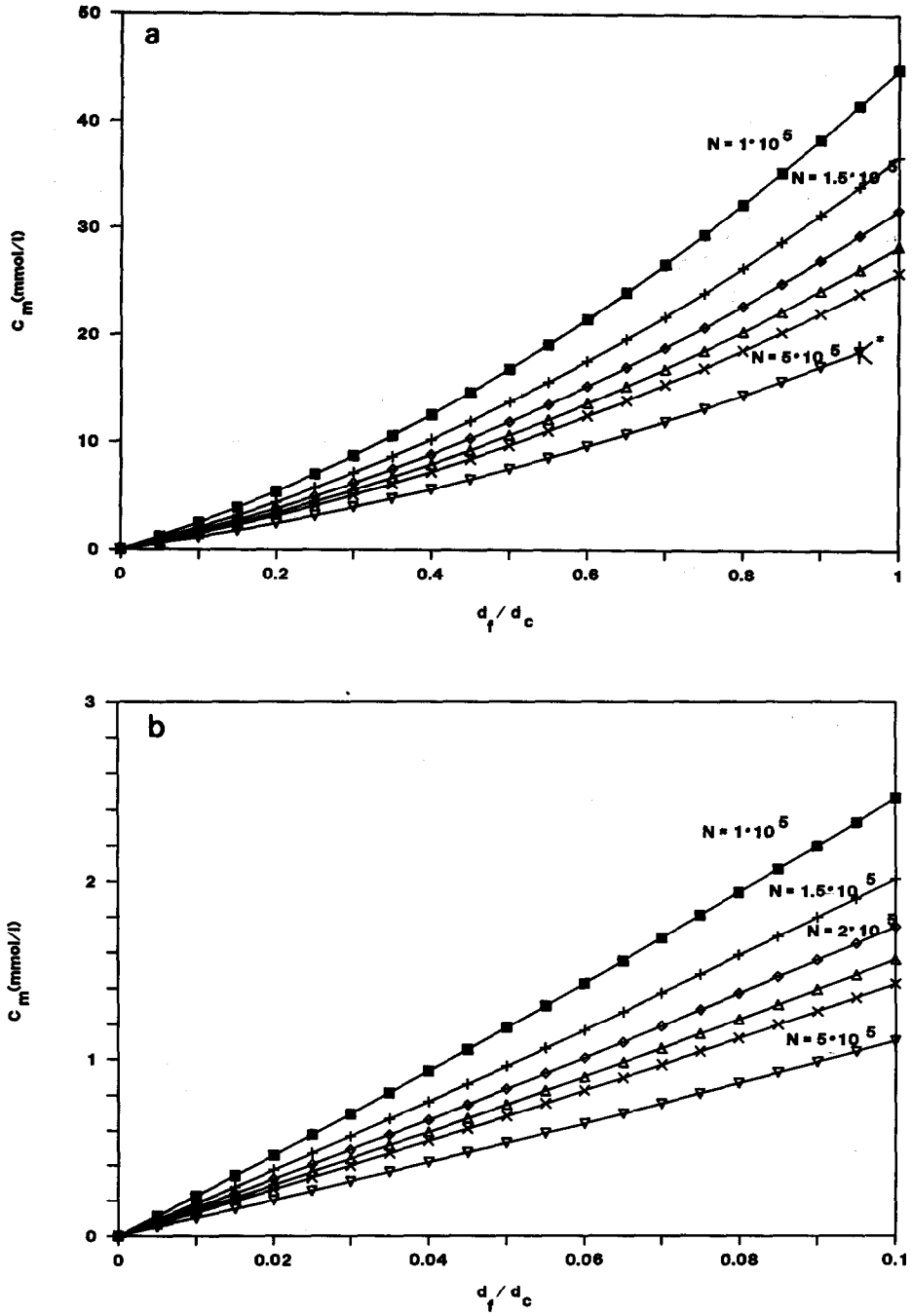

Fig. 7. Eluting concentration C_m (mmol/l) *versus* d_f/d_c ratio. (a) For the liquid–liquid system with $t_m = 1000$ s, $\Delta P = 20$ MPa and various N values: ■ = $1 \cdot 10^5$; + = $1.5 \cdot 10^5$; ◇ = $2 \cdot 10^5$; △ = $2.5 \cdot 10^5$; × = $3 \cdot 10^5$; ▽ = $5 \cdot 10^5$. (b) For the silicone system with $t_m = 1000$ s, $\Delta P = 20$ MPa and various N values: ■ = $1 \cdot 10^5$; + = $1.5 \cdot 10^5$; ◇ = $2 \cdot 10^5$; △ = $2.5 \cdot 10^5$; × = $3 \cdot 10^5$; ▽ = $5 \cdot 10^5$.

system. This demonstrates again the importance of having a high diffusion coefficient in the stationary layer. In Fig. 7a the curve of C_m is linear from $d_f/d_c = 0$ to 0.1, and in this region the phase ratio can be approximated by 4 times the d_f/d_c ratio, but for larger d_f/d_c ratios the phase ratio had to be calculated with 4 times $d_f/d_c + (d_f/d_c)^2$. For the liquid–liquid system only the latter equation for the phase ratio had to be used.

Dependence of C_m and the maximum M_{pl} on the efficiency

As mentioned above, C_m and the maximum M_{pl} depend very strongly on the efficiency. The maximum M_{pl} and subsequently C_m were calculated for the liquid–liquid system and the silicone system for $N = 1 \cdot 10^4$–$1 \cdot 10^6$. In Fig. 8 it can be seen that the two curves are identical for both systems, but M_{pl} for the liquid–liquid system is about ten times larger than that for the silicone system. In this plot it is obvious that the loadability is extremely sensitive to the number of plates needed in the chromatographic system. Increasing N means a decrease in M_{pl}; an increase in N of one order of magnitude gives a decrease in M_{pl} of three orders of magnitude.

In Fig. 9 it can be seen that for C_m, at maximum M_{pl}, the same conclusion as mentioned above can be drawn, except that C_m for the liquid–liquid system is about 15 times larger than that for the silicone system. An increase in N by a factor of 10 decreases C_m by a factor of the square root of 10.

Packed capillaries versus open-tubular columns

It is interesting to compare the loadabilities obtained with those obtained with the so-called micro-packed capillaries. Such columns, as studied by Novotny and

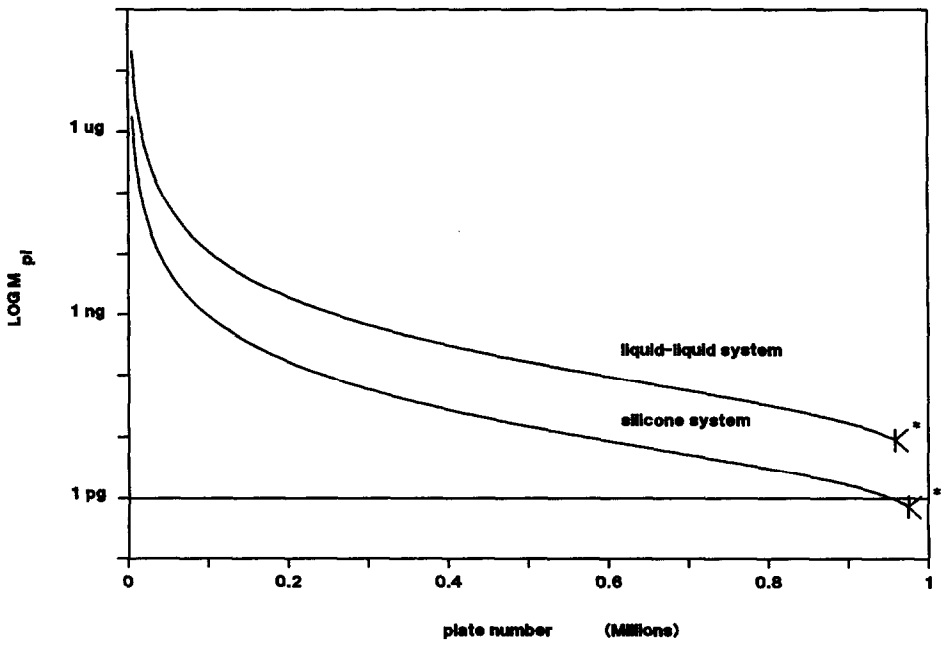

Fig. 8. Maximum mass loadability M_{pl} (pg) on a log scale *versus* N for the liquid–liquid system and the silicone system, with $t_m = 1000$ s and $\Delta P = 20$ MPa.

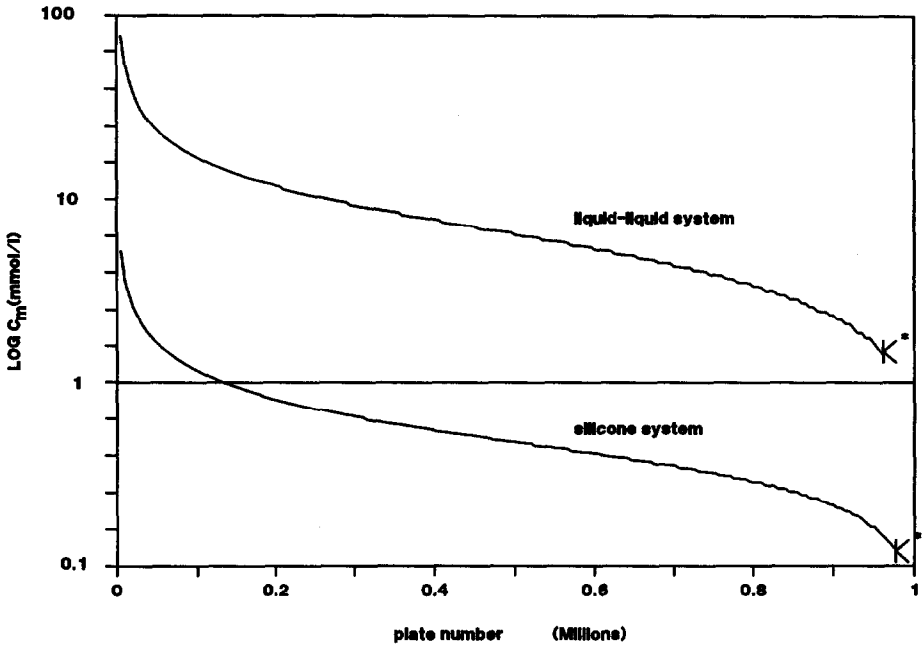

Fig. 9. Eluting concentration C_m (mmol/l), at maximum loadability, on a log scale *versus* N for the liquid–liquid system and the silicone system, with t_m = 1000 s and ΔP = 20 MPa.

co-workers[25–27] and more recently by Kennedy and Jorgenson[28], aim at the realization of higher speeds and accessible plate counts by exploiting the smaller packing density and associated better permeabilities and separation impedances. The value of the latter may also be significantly improved by the smaller h values [down to 1 (ref. 28)], giving an additional improvement of a factor of 4. Altogether, separation impedances $E = h^2\varphi$ as low as 500 have been observed[28,29]. The open-tubular columns found in this work to be optimum have E values (*e.g.*, the second entry in Table II) of $32 \cdot h^2 = 220$, *i.e.*, in the same range.

The mentioned kinetic performance of micro-packed capillary columns can only be realized if the ratio of the particle to the tube diameter is very low, of the order of 5. As particle sizes of about 5 μm are indicated, a tube diameter of 25 μm is a good average if E values of 500 are to be obtained. The sample capacity is therefore also very low and it will be compared with our results.

The first point is to find the operating point generating $3 \cdot 10^5$ plates in 1000 s (t_m). With d_p = 5 μm and $D_m = 10^{-9}$ m^2/s, this condition indicates that H/v = 0.0033 s = $d_p^2/D_m \cdot h/v$, *i.e.*, h/v = 0.132. Taking one of Kennedy and Jorgenson's columns (Fig. 3a in ref. 28), one can intersect the $h = 0.132\,v$ line with the observed h–v dependence. One then finds $h_{oper} \approx 1.3$, $v_{oper} = 10$ (21-μm d_c column). In such a column, having the required kinetic performance, the volume of porous silica in one plate is

$$\pi/4 \cdot d_c^2 H \varepsilon_{SiO_2} = \pi/4 \cdot d_c^2 h d_p \varepsilon_{SiO_2} = 1.4 \cdot 10^{-15}\,\mathrm{m}^3$$

(with d_c = 21 μm, d_p = 5 μm and ε_{SiO_2} = 0.6).

In the open-tubular LC column, the second entry in Table II, we have a volume of porous silica in one plate of

$$\pi/4(d_b^2 - d_c^2)H = 6.9 \cdot 10^{-16}\ \mathrm{m}^3$$

(with $H = 12.9\ \mu\mathrm{m}$, $d_b = 9.56\ \mu\mathrm{m}$ and $d_c = 4.90\ \mu\mathrm{m}$).

It follows that the mass loadability when the surface areas in both types of silica are the same differ by only a factor of two. The conclusion is that the range of application, detection and injection problems, etc., will be virtually the same for both types of chromatography. A similar conclusion was also drawn by Guiochon[30]. However, open-tubular LC colunns have much greater potential for further kinetic improvements on further miniaturization. On the other hand, it has to be admitted that Kennedy and Jorgenson[28] demonstrated their type of columns experimentally, while the thick-film 5-μm open tube, entry 2 in Table II, has not yet been realized.

CONCLUSIONS

Changes in N have a very strong influence on M_{pl}, whereas changes in t_m and ΔP have a strong and a weak influence, respectively, on M_{pl}. A 10-fold increase in N means a decrease of a factor of 1000 in M_{pl}.

The maximum column length for the fixed input specifications is about 5 m for all the mentioned phase systems.

The d_f/d_c ratio at maximum loadability for the liquid–liquid system is 10 times larger than for the silicone system, which can be explained by the expression $\sqrt{(D_{s1}/D_{s2})}$. The use of a phase system with a very small diffusion coefficient in the stationary phase is unfavourable with respect to mass loadability.

The plate-height equation for the liquid–liquid system at maximum M_{pl} is $h = 2/v + 0.133v$ and for the silicone system $h = 2/v + 0.115v$. This is an increase in C of 60% (the liquid–liquid system) and 50% (the silicone system) compared with C for very thin films ($h = 2/v + 0.08v$).

The monolayer system has a M_{pl} which is about $2 \cdot 10^6$ smaller than that for the liquid–liquid system.

C_m can only be influenced by the d_f/d_c ratio and N. For the liquid–liquid system C_m is about 15 times larger than for the silicone system.

The calculated M_{pl} of a 21-μm I.D. micro-packed capillary column and an open-tubular LC column (second entry in Table II) are in the same range. However, it should be pointed out that the thick-film 5-μm open-tubular LC column has not yet been realized.

SYMBOLS

D_m	diffusion coefficient in the mobile phase ($D_m = 1 \cdot 10^{-9}\ \mathrm{m}^2/\mathrm{s}$)
D_s	diffusion coefficient in the stationary phase (liquid–liquid system, $D_s = 5 \cdot 10^{-10}\ \mathrm{m}^2/\mathrm{s}$; silicone system, $D_s = 7 \cdot 10^{-12}\ \mathrm{m}^2/\mathrm{s}$)
d_c	diameter of the cross-section of the mobile phase in the column (μm)
d_f	film thickness of the stationary phase (μm)
h	reduced plate height

k'	capacity factor ($k' = 3$)
L	column length (m)
M_{pl}	mass loadability in one plate, equal to the amount of stationary phase in one plate (pg)
N	number of theoretical plates
ΔP	pressure drop across the column (MPa)
v	reduced velocity
η	viscosity of the mobile phase ($\eta = 1 \cdot 10^{-3}$ Pa s)
φ	pressure resistance factor (open tube: $\varphi = 32$)
δ_f	reduced film thickness
ρ_{sf}	density of stationary phase ($\rho_{sf} = 1 \cdot 10^6$ g/m^3)
t_m	dead time of the mobile phase (s)
C_m	eluting concentration (mmol/l)
MW	molecular weight of solute (MW = 200 g/mol)
m_{30}	reduced load that corresponds to a 30% increase in peak width ($m_{30} = 2$)
$\alpha_{OH(s)}$	surface concentration of the accessible silanols (4 μmol/m^2)
$F(k')_m$, $F(k')_s$	functions of k'

REFERENCES

1 J. H. Knox and M. T. Gilbert, *J. Chromatogr.*, 186 (1979) 405.
2 J. H. Knox and M. Saleem, *J. Chromatogr. Sci.*, 7 (1969) 614.
3 J. Jorgenson and E. J. Guthrie, *J. Chromatogr.*, 255 (1983) 335.
4 H. P. M. van Vliet and H. Poppe, *J. Chromatogr.*, 346 (1985) 149.
5 L. A. Knecht, E. J. Guthrie and J. Jorgenson, *Anal. Chem.*, 56 (1984) 479.
6 S. Folestad, B. Josefsson and M. Larsson, *J. Chromatogr.*, 391 (1987) 347.
7 O. van Berkel, J. C. Kraak and H. Poppe, *Chromatographia*, 24 (1987) 739.
8 P. R. Dluzneski and J. W. Jorgenson, *J. High Resolut. Chromatogr. Chromatogr. Commun.*, 11 (1988) 332.
9 O. van Berkel-Geldof, J. C. Kraak and H. Poppe, *J. Chromatogr.*, 499 (1990) 345.
10 H. Poppe, J. C. Kraak, O. van Berkel-Geldof and P. P. H. Tock, in P. Sandra (Editor), *Proceedings of Ninth Congress on Capillary Chromatography, Monterey, 1988*, Hüthig, Heidelberg, p. 345.
11 P. P. H. Tock, G. Stegeman, R. Peerboom, H. Poppe, J. C. Kraak and K. K. Unger, *Chromatographia*, 24 (1987) 617.
12 P. P. H. Tock, C. Boshoven, H. Poppe, J. C. Kraak and K. K. Unger, *J. Chromatogr.*, 477 (1989) 95.
13 M. D. Oates and J. W. Jorgenson, *Anal. Chem.*, 61 (1989) 432.
14 R. T. Kennedy and J. W. Jorgenson, *Anal. Chem.*, 61 (1989) 436.
15 M. J. E. Golay, in H. Desty (Editor), *Gas Chromatography 1958*, Butterworths, London, 1958, pp. 36–55.
16 L. S. Ettre, *Chromatographia*, 17 (1983) 553.
17 C. A. Cramers, *J. High Resolut. Chromatogr. Chromatogr. Commun.*, 9 (1986) 676.
18 Th. Noy, J. Curvers and C. Cramers, *J. High Resolut. Chromatogr. Chromatogr. Commun.*, 9 (1986) 753.
19 R. T. Ghijsen and H. Poppe, *J. High Resolut. Chromatogr. Chromatogr. Commun.*, 11 (1988) 271.
20 J. C. Giddings, S. L. Seager, L. R. Stucki and G. H. Stewart, *Anal. Chem.*, 32 (1960) 867.
21 H. Poppe and J. C. Kraak, *J. Chromatogr.*, 255 (1983) 395.
22 P. J. Schoenmakers, *J. High Resolut. Chromatogr. Chromatogr. Commun.*, 11 (1988) 271.
23 J. E. Eble, R. L. Grob, P. E. Antle and L. R. Snyder, *J. Chromatogr.*, 384 (1987) 25.
24 R. T. Ghijsen, H. Poppe, J. C. Kraak and P. P. E. Duysters, *Chromatographia*, 27 (1989) 60.
25 T. Tsuda and M. Novotny, *Anal. Chem.*, 50 (1978) 271.
26 V. L. McGuffin and M. Novotny, *J. Chromatogr.*, 255 (1983) 381.
27 K. E. Karlsson and M. Novotny, *Anal. Chem.*, 60 (1988) 1662.
28 R. T. Kennedy and J. W. Jorgenson, *Anal. Chem.*, 61 (1989) 1128.
29 C. Borra, M. Soon and M. Novotny, *J. Chromatogr.*, 385 (1987) 75.
30 G. Guiochon, *Anal. Chem.*, 53 (1981) 1318.